Chemical Physics Letters 499 (2010) 193–198

Contents lists available at ScienceDirect

Chemical Physics Letters

journal homepage: www.elsevier.com/locate/cplett

Topological study of bis(cyclopentadienyl) titanium and bent titanocenes

Caio L. Firme [a,*], Daniel de L. Pontes [a], Octávio A.C. Antunes [b,1]

[a] Federal University of Rio Grande do Norte, Department of Chemistry, Av. Salgado Filho, s/n, Lagoa Nova, Natal/RN, CEP 59000-000, Brazil
[b] Universidade Federal do Rio de Janeiro, Instituto de Química, Av. Athos da Silveira Ramos, 149, CT Bloco A, 6° andar, Cidade Universitária – Ilha do Fundão, Rio de Janeiro, BR 21941-909, Brazil

ARTICLE INFO

Article history:
Received 4 July 2010
In final form 15 September 2010
Available online 18 September 2010

ABSTRACT

The electronic nature of ferrocene, titanocene and some bent titanocenes was analyzed by QTAIM. PBE1PBE-optimised geometrical data agreed well with X-ray diffraction data, this method being chosen to extract and analyze the wave functions of all studied metallocenes within the QTAIM framework. Within the studied metallocenes, the number of bond paths can be used as an indicative of their stability. The $Ind_2Ti(CH_3)_2$ has less Ti–C bond paths than the $Cp_2Ti(CH_3)_2$ as well as the Cp_2Ti has less C–Mt bond paths than Cp_2Fe. These results concords with the smaller stabilities of $Ind_2Ti(CH_3)_2$ and Cp_2Ti relative to their counterparts.

1. Introduction

Metallocenes are compounds containing a transition metal and two η^5 cyclopentadienyl (Cp) ligands in a sandwich structure where the two cyclopentadienyl anions are coplanar with equal bond lengths and strengths [1,2]. Metallocenes having group 4–7 transition metals are capable of binding up to three ligands in addition to both Cp groups. These compounds are called bent metallocenes because the Cp groups bend back away from the ligands. The d^2 $[Cp_2Ti]^{+2}$ fragment can bind two chlorine atoms to give Cp_2TiCl_2 with 16 electrons and an empty orbital in Ti atom [1,3].

Group 4 bent metallocenes activated by methylaluminoxane (MAO) co-catalyst form a well-known highly active catalytic system for olefin polymerization [4–6]. The reaction between these bent metallocenes and co-catalyst molecules generates aluminoxane anions and metallocene cations, which are the true polymerization active species [7]. Bent metallocenes from the group 4 have pseudotetrahedric geometry coordinated by two substituted or non-substituted π ligand cyclopentadienyl groups and two σ groups [8–11]. In these catalysts, the π bonded ligands strongly influence the stereo- and regioregularity of the produced polymers [12–16]. Chlorine and methyl σ-bonded groups do not affect the stereo- and regioregularity of the produced polymers via bent metallocene catalysts. However, voluminous σ-bonded alcoholato ligands can affect either the molecular weight or the regioregularity of the produced polypropylenes [17–20].

Molecular orbital (MO) and experimental studies of bent metallocenes have been done by different research groups [21–25]. Nevertheless, topological analysis is needed for better understanding of the electronic nature of these important catalysts for olefin polymerization. The quantum theory of atoms in molecules (QTAIM) has been used to study coordination compounds, including metallocenes [24–27]. In this work we study the topology of bis(cyclopentadienyl) iron, bis(cyclopentadienyl) titanium and different bent titanocenes and we establish a relation between C–Mt (where Mt = Ti, Fe) bond paths and their stabilities.

2. Computational details

The geometries of the studied species were optimized by using standard techniques [28]. Vibrational analysis on the optimized geometries of selected points of the potential energy surface was carried out in order to determine whether the resulting geometries are true minima or transition states, by checking the existence of imaginary frequencies. The calculations were performed at PBE1PBE/6-311++G(2d,2p) level [29–31] by using Gaussian 03 package [32]. The electronic density was derived from the Kohn–Sham orbitals obtained at both levels and further used for QTAIM calculations by means of AIM2000 software [33]. For comparison reasons, the topological data were also obtained from B3LYP/6-311++G(2d,2p)/QTAIM calculations whose results were similar to those from PBE1PBE/6-311++G(2d,2p)/QTAIM calculations.

3. QTAIM

Topological analysis of QTAIM is based on the distribution of electronic density. In QTAIM the molecular system is divided into subsystems called atomic basins. Each atomic basin contains the nucleus, core and valence electrons. The atomic basins are obtained in terms of a property of the gradient vector of the charge density ($\nabla\rho$). The quantum condition of the subsystem states that

* Corresponding author.
E-mail addresses: firme.caio@gmail.com, caiofirme@quimica.ufrn.br (C.L. Firme).
[1] In memoriam.

0009-2614/$ - see front matter © 2010 Elsevier B.V. All rights reserved.
doi:10.1016/j.cplett.2010.09.038

the surface bounding the subsystem shall not be crossed by any gradient vectors of charge density (ρ). Quantum observables can be calculated within each atomic basin. As a consequence, a molecular property can be obtained by summing the corresponding atomic property of all atoms of the molecule. The critical points of the charge density are obtained where $\nabla\rho = 0$. The bond critical point (BCP) is a saddle point between each bonding atomic pair [34,35]. The Laplacian of the charge density ($\nabla^2\rho$) is the sum of the three eigenvalues of the Hessian matrix of the charge density (λ_1, λ_2 and λ_3) [34]. The negative sign of the $\nabla^2\rho$ represents concentration of the charge density and the positive sign of the $\nabla^2\rho$ represents charge depletion.

The type of chemical bond or interaction between two atoms can be classified according to the value of the charge density of the critical point (ρ_b), the value and the sign of the Laplacian of the charge density, the ratio $|\lambda_1|/\lambda_3$and the total energy density (H_b) at the CP. When $\nabla^2\rho > 0$, ρ_b is relatively low ($\rho_b < 6 \times 10^{-2}$ au.), the ratio $|\lambda_1|/\lambda_3 < 1$ and H_b has a positive value, close to zero, the chemical interaction is defined as closed shell and it is applied to hydrogen bond, ionic bond and van der Waals interactions [34]. When the order of magnitude of the ρ_b is 10^{-1}, $\nabla^2\rho < 0$, the ratio $|\lambda_1|/\lambda_3 > 1$ (close to one for single bonds) and H_b has a negative value, there is a covalent bond involving this bond critical point.

The delocalization index (DI) is the amount of shared electrons between each atomic pair and it is derived from the Fermi hole density [36,37]. The localization index (LI) is the amount of non-shared electrons within each atomic basin [36,37]. It is important to emphasize that QTAIM is based on a quantum observable and its topological analysis is a powerful tool for the interpretation of X-ray determined charge densities [38–40].

4. Rationale

Our previous work considering the relation between DI and formal bond order [41] has shown implicitly that Lewis model [42] has limitations within the quantum world of the electronic distribution. In Lewis model, single, double and triple bonds have two, four and six electrons in a valence bonding region, respectively, regardless the Coulombic and Fermi repulsions among them.

Our work [41] has shown that there is a correspondence between QTAIM and Lewis model since we found a linear relation between DI and formal bond order, for different bonding atomic pairs. Nonetheless, the DI calculations indicate that there are actually one, two and three shared electrons, in average, for single, double and triple bonds, respectively. This discrepancy is because QTAIM is based on quantum physics while the Lewis model is based on an empirical (though useful) model which neglects all kinds of electronic repulsions.

Although the 16 and 18-electron rule, introduced by Nevil Sidgwick in 1923, has consistency with a large body of experimental evidences [43], it is an empirical rule based on Lewis model. Then, it is plausible that QTAIM and the 16 and 18-electron rule will not agree exactly on the quantity of shared electrons between the transition metal atom and each donor atom from ligands in coordination compounds.

5. Results and discussion

5.1. Bis(cyclopentadienyl) titanium

Although bis(cyclopentadienyl) iron (Cp_2Fe) and bis(cyclopentadienyl) titanium (Cp_2Ti) are not applied directly to polymerization catalysis, the knowledge of their topology is important for a topological comparison with its bent parents of common use in polymerization process.

The bis(cyclopentadienyl) iron compound can present two possible structures, eclipsed (D_{5h} symmetry group) and staggered (D_5 point group). In the Figure 1A we have the most stable conformation (D_{5h}) where the cyclopentadienyl ligands are parallel to each other, carbon–hydrogen bonds are eclipsed and all C–Fe bonds have the same bond length. However, observing the Cp_2Ti geometry, one can see that the cyclopentadienyl groups are not exactly parallel to each other and the C–Ti and C–C bond lengths are not uniform (Figure 1C).

The molecular graphs of Cp_2Fe and Cp_2Ti follow Poincaré-Hopf rule ($n-b+r-c+1$), where n is the number of nuclear attractors, b is the number of bond critical points, r is the number of ring critical points, and c is the number of cage critical points [44]. The bond paths of these molecular graphs are mirrored by their corresponding virial paths, where the potential energy density is maximally negative [45]. In the case of molecular graph of Cp_2Ti, although it has additional ring critical points (RCP) and cage critical points (CCP), we think it has no additional bond path because its virial graph shows only two Ti–C virial paths for each cyclopentadienyl group and it shows no additional RCP and CCP.

The values of charge density of the BCP, the Laplacian of the charge density and the total energy density indicate that there is a closed shell interaction in the Ti–C atomic pairs. The number of shared electrons in Ti–C bonds is not uniform and it follows the same trend of their bond lengths (or interatomic distances). The molecular graph of bis(cyclopentadienyl) titanium has only two bond paths between Ti and each Cp ligand. These bond paths are related to the smallest Ti–C interatomic distances in bis(cyclopentadienyl) titanium, i.e., the smallest Ti–C interatomic distances have corresponding bond paths.

The DI results in Figure 1 show that Ti–C2 and Ti–C3 atomic pairs, where there is no bond path between each of these atomic pairs, have smaller amount of shared electron than that from Ti–C1 atomic pair. The DI values in Ti–C2 and Ti–C3 atomic pairs represent 73% and 60%, respectively, from that in Ti–C1 atomic pair.

It is known from the literature that bis(cyclopentadienyl) iron is more stable than bis(cyclopentadienyl) titanium towards solvent stability [46,47]. From the QTAIM perspective, the number of bond paths, presented by each metallocene studied on this work, is in accordance with their stability behavior since $(Cp)_2Fe$ compound has five Fe–C bond paths for each cyclopentadienyl ring while the $(Cp)_2Ti$ has only two Ti–C bond paths for each cyclopentadienyl ligand. From the geometric perspective, all Fe–C interatomic distances in $(Cp)_2Fe$ have the same value (Figure 1A) while Ti–C in $(Cp)_2Ti$ have different values, resulting in a higher symmetry of bis(cyclopentadienyl) iron and higher number of bond paths.

Possibly, the number of bond paths between metal atom and carbon atoms of the π-ligands can be used as an indicative of metallocene stability. To reinforce this proposal we can see that the values of the delocalization index and the charge density of BCP in Fe–C bond are higher than those from Ti–C bond (Figure 1). Furthermore, the electronic energy values obtained from PBE1PBE calculations of optimized structures in Table 1 shows that the synthesis reaction of Cp_2Fe, which has more C–Mt bond paths than those in Cp_2Ti (where Mt is Fe or Ti), is more exothermic than that to obtain Cp_2Ti.

5.2. Bent titanocenes

In this section we analyze the topology of some important bent titanocenes applied to olefin polymerization catalysis. We also analyze the topology of the cationic titanocene since it is recognized as the effective catalyst in olefin polymerization via metallocene compounds.

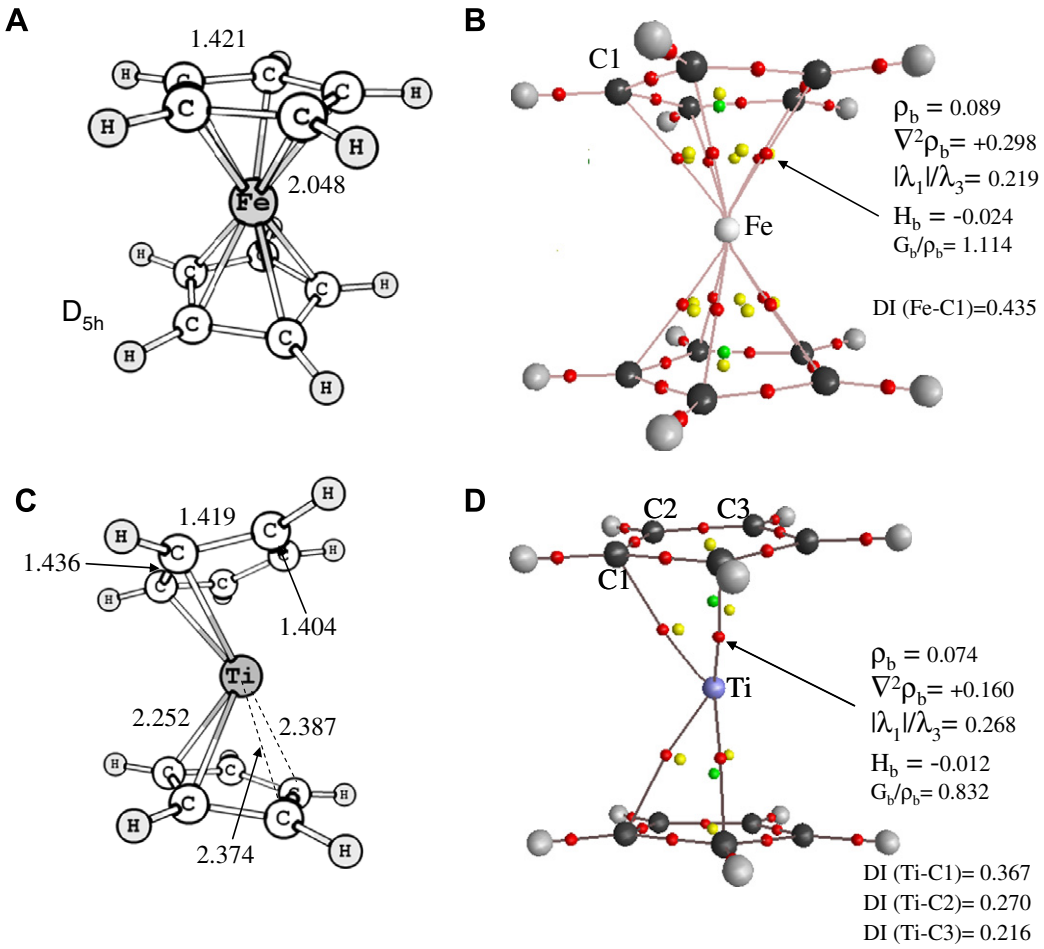

Figure 1. Selected bond lengths (in Angstroms), point group symmetry (A) and molecular graph (B) of bis(cyclopentadienyl) iron. Selected bond lengths (C) and molecular graph (D) of bis(cyclopentadienyl) titanium. Dashed lines represent interatomic distances; DI is the delocalization index between metal and C atoms; ρ_b is the charge density; $\nabla^2\rho_b$ is Laplacian of the charge density; H_b is the energy density, in au.; $|\lambda_1|/\lambda_3$ is the ratio of eigenvalues of Hessian matrix of the charge density from bond critical points and G_b/ρ_b is the ratio between kinetic energy density and charge density of bond critical point. Green, yellow and red dots represent (3,+3), (3,+1) and (3,−1) critical points, respectively. (For interpretation of the references to colour in this figure legend, the reader is referred to the web version of this article.)

Table 1
Values of electronic energy change of reaction (in kcal/mol) from the synthesis reaction of Cp_2Ti and Cp_2Fe and their corresponding relation with the number of bond paths between each π-ligand and Ti/Fe atom.

Reaction	Number of bond paths between each π-ligand and Ti/Fe atom	Electronic energy change of reaction (kcal/mol)
$TiCl_2 + 2CpLi \rightarrow Cp_2Ti + 2\ LiCl$	2	−41.3
$FeCl_2 + 2CpLi \rightarrow Cp_2Fe + 2\ LiCl$	5	−88.0

Figure 2 shows selected bond lengths (in Å) and the approximate point group symmetries of dimethyl-bis(cyclopentadienyl) titanium, $[Cp_2Ti(CH_3)_2]$, methyl-bis(cyclopentadienyl) titanium cation, $[Cp_2Ti(CH_3)]^+$ and dimethyl-bis(indenyl) titanium, $[Ind_2Ti(CH_3)_2]$. No constraint to point group symmetries was imposed for the optimization procedure. Figure 2 also shows the bond lengths of $Ind_2Ti(CH_3)_2$ from X-ray diffraction results obtained by Atwood and coworkers [48]. Comparing the bond lengths, we can observe a good agreement between experimental results and computational geometric parameters found for the indenyl compound. This agreement indicates that PBE1PBE is an appropriate density functional methodology to study titanocenes.

When going from neutral dimethyl-bis(cyclopentadienyl) titanium to its corresponding cationic form, one can see that the bond length Ti–C (methyl group) decreases considerably (Figure 2) while the delocalization index and the charge density of the BCP in Ti–C (methyl group) bond increase (Figure 3). This observation can be attributed to the fact that Ti atom in the cationic form is more electronically deficient.

Figure 3 shows the molecular graphs of $Cp_2Ti(CH_3)_2$ and $[Cp_2Ti(CH_3)]^+$. Some of their corresponding topological information also are depicted in Figure 3. All molecular graphs follow Poincaré-Hopf rule.

The values of charge density of BCP (ρ_b), the Laplacian of ρ_b ($\nabla^2\rho_b$) and of the ratio $|\lambda_1|/\lambda_3$ indicate that all bond paths between Ti and C atoms, from cyclopentadienyl ligands, have closed shell interactions (ionic interaction). However, the values of the kinetic energy density/charge density ratio (G_b/ρ_b) and of the energy density of the BCP (H_b) do not correspond to those from closed shell interaction [34]. Then, these Ti–C (from cyclopentadienyl) interactions are intermediate between closed shell and shared interactions, being closer to closed shell interaction.

In the case of the bond critical point (BCP 4) between Ti and C4 (from methyl group) atoms all topological data are characteristic of an intermediate interaction between ionic and covalent bond. One can see that its $\nabla^2\rho_b$ is less positive (lower charge dispersion); its H_b is more negative (more stable); and its ρ_b is higher than those from Ti–C bond paths involving cyclopentadienyl carbon atoms (BCP's 1–3). Moreover, the QTAIM atomic charge of the methyl

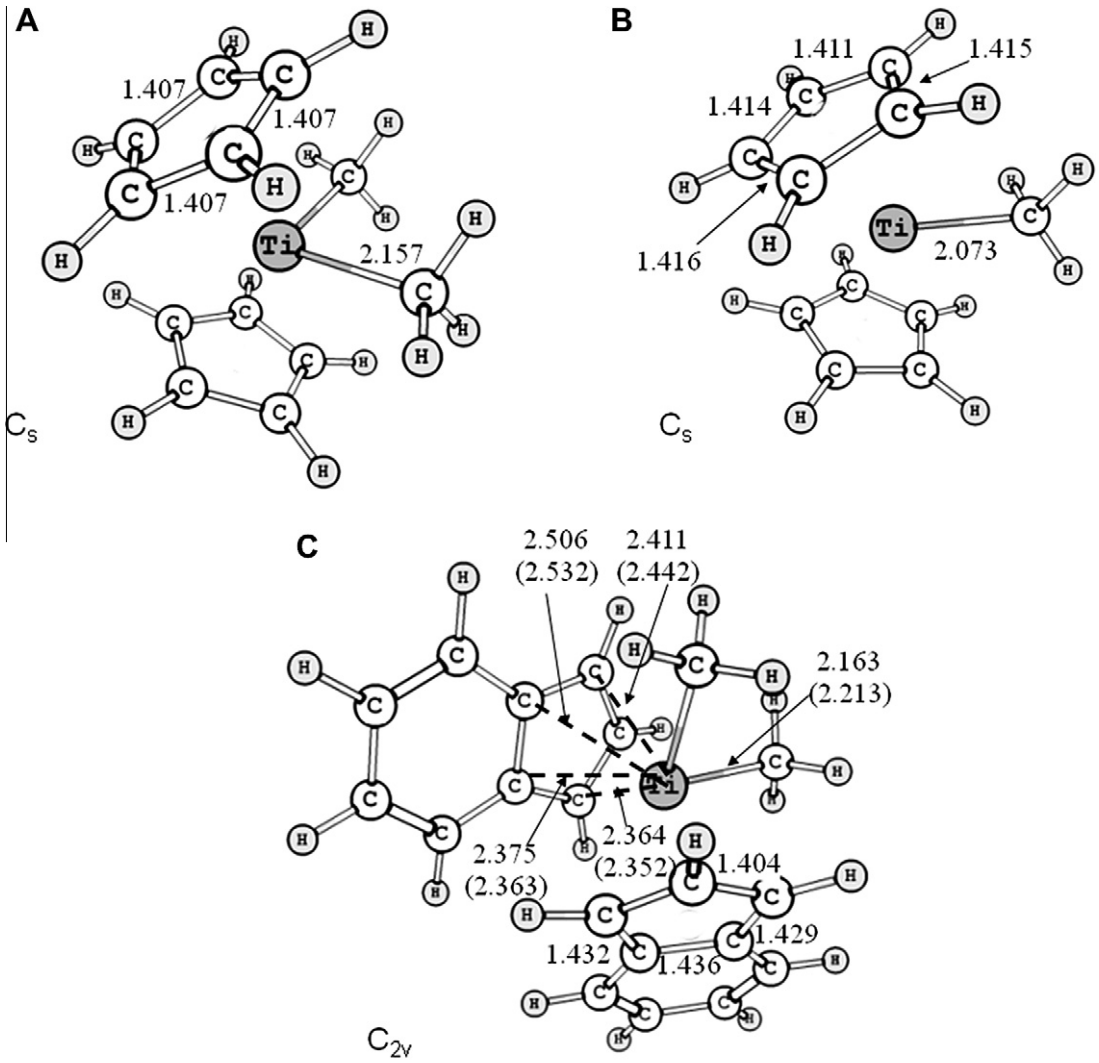

Figure 2. Selected bond lengths (in Angstroms) and point group symmetry of $Cp_2Ti(CH_3)_2$ (A), $[Cp_2Ti(CH_3)]^+$ (B), and $Ind_2Ti(CH_3)_2$ (C), whose bond lengths between parentheses are from experimental X-ray diffraction data [48]. Dashed lines represent interatomic distances.

carbon is much more negative than the atomic charges of the cyclopentadienyl carbon atoms, which means that more charge transfer occurred to methyl carbon than to cyclopentadienyl carbon atoms.

Thus, an individual bond from the set of interactions between cyclopentadienyl ligand and Ti atom is smaller than that involving the σ-methyl ligand and Ti atom. In addition, the DI values between Ti and C4 atoms are twofold up to threefold higher than those between Ti atom and C atom of cyclopentadienyl ligand. This result is in accordance with experimental expectations since π ligands are more labile than σ ligands.

Molecular graphs of $Cp_2Ti(CH_3)_2$ and $[Cp_2Ti(CH_3)]^+$ show that there are three bond paths between Ti atom and C atoms of cyclopentadienyl ligand. In $[Cp_2Ti(CH_3)]^+$ there is one interaction atomic line involving Ti and C atoms (from cyclopentadienyl ligand) which it is not mirrored by the corresponding virial path of $[Cp_2Ti(CH_3)]^+$ and it is not an actual bond path.

In both $Cp_2Ti(CH_3)_2$ and $[Cp_2Ti(CH_3)]^+$ there are some Ti–C atomic pairs which do not have bond paths linking them. However, these atomic pairs have considerable DI values which are just a bit smaller than those from Ti–C atomic pairs with bond paths (compare DI values from Ti–C5 and Ti–C3 atomic pairs in Figure 3). It is worth mentioning that atomic charges and atomic energies of cyclopentadienyl carbon atoms which have bond path with Ti atom are more negative and smaller, respectively, than those which do not have bond path with Ti atom (see Figure 3). Then, although the small difference of DI values between Ti–C atomic pairs (with or without bond paths) in $Cp_2Ti(CH_3)_2$, the carbon atoms linked to Ti atom by bond path are more stable than those without Ti–C bond path.

From neutral titanocene $Cp_2Ti(CH_3)_2$ to cationic titanocene $[Cp_2Ti(CH_3)]^+$, there is an increase of charge density in bond critical points linking carbon atom (from cyclopentadienyl ligand and methyl group) and titanium atom. There is also an increase in the number of shared electrons (DI values) between Ti and C atoms from neutral titanocene to cationic titanocene. Then, the reaction between the neutral bent titanocene and an aluminium-based compound (co-catalyst in coordination polymerization) yields a cationic titanocene whose remaining Ti–C chemical interactions are stronger than those from neutral titanocene.

Figure 4 shows the molecular graph and virial graph of dimethyl-bis(indenyl) titanium, $Ind_2Ti(CH_3)_2$, and some of its topological information. The molecular graph follows Poincaré-Hopf rule. The indenyl ligand has a different characteristic from cyclopentadienyl ligand: it tends to slip from η^5 to η^3 more easily than cyclopentadienyl ligand because the full aromatic stabilization of the benzo ring is restored in the slipped form [1].

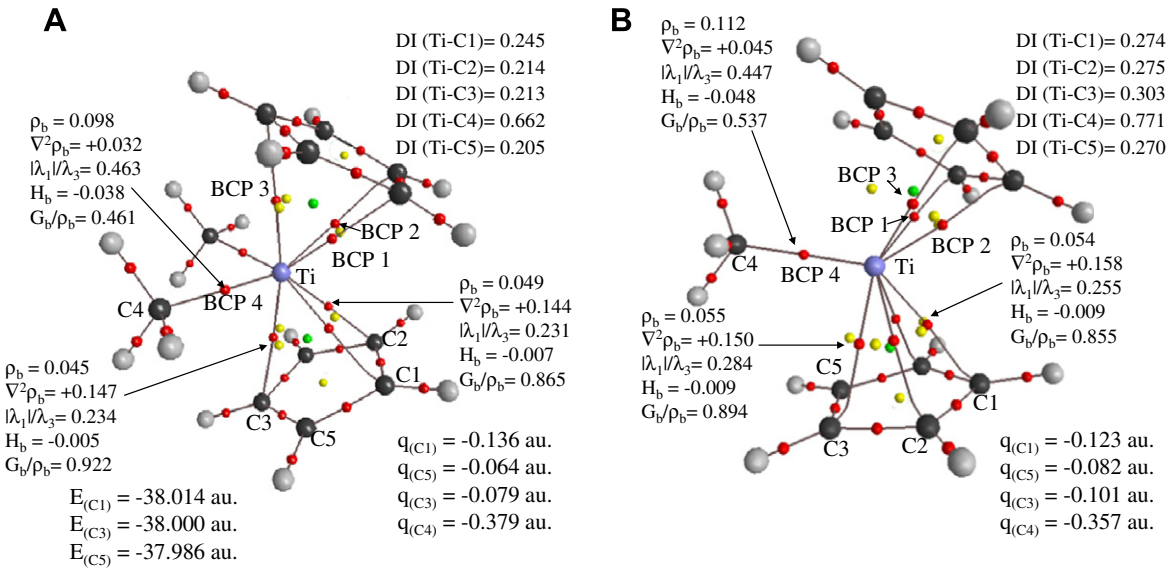

Figure 3. Molecular graphs of $Cp_2Ti(CH_3)_2$ (A) and $[Cp_2Ti(CH_3)]^+$ (B). The delocalization index (DI) values between Ti and C atoms. The charge density (ρ_b), Laplacian of the charge density ($\nabla^2\rho_b$), energy density (H_b), atomic energy (E), QTAIM atomic charge (q), in au., the ratio $|\lambda_1|/\lambda_3$ of the bond critical points and G_b/ρ_b is the ratio between kinetic energy density and charge density of bond critical point. Green, yellow and red dots represent (3,+3), (3,+1) and (3,−1) critical points, respectively (For interpretation of the references to colour in this figure legend, the reader is referred to the web version of this article.).

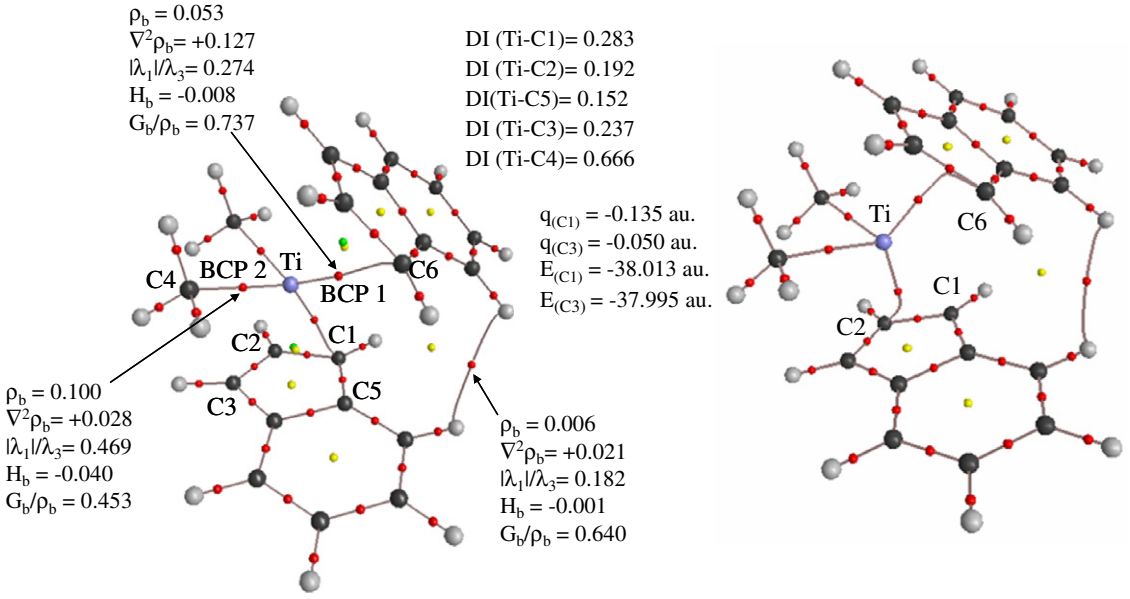

Figure 4. Molecular graph (to the left) and virial graph (to the right) of $Ind_2Ti(CH_3)_2$. The delocalization index (DI) between Ti and C atoms. The charge density (ρ_b), Laplacian of the charge density ($\nabla^2\rho_b$), the energy density (H_b), atomic energy (E), QTAIM atomic charge (q), in au., the ratio $|\lambda_1|/\lambda_3$ of the bond critical points and G_b/ρ_b is the ratio between kinetic energy density and charge density of bond critical point. Green, yellow and red dots represent (3,+3), (3,+1) and (3,−1) critical points, respectively (For interpretation of the references to colour in this figure legend, the reader is referred to the web version of this article.).

In Figure 4, the analysis of the values of ρ_b, $\nabla^2\rho_b$ and $|\lambda_1|/\lambda_3$ of the bond paths between Ti and C atoms (from indenyl ligands) are characteristic of closed shell interactions. However, the values of G_b/ρ_b and H_b do not correspond to those from closed shell interaction. Then, these Ti–C (sp^2) interactions are intermediate between closed shell and shared interactions, being closer to closed shell interaction. In the case of the Ti–C(methyl group) atomic pair (BCP 2), all topological data indicate that this bond is intermediate between ionic and covalent interactions.

Thus, one Ti–C chemical interaction from σ-methyl ligand is stronger than that from one Ti–C chemical interaction from π-indenyl ligand.

Molecular graph of $Ind_2Ti(CH_3)_2$ shows just one bond path between each indenyl group and Ti atom (Figure 4). However, there are one ring critical point and one cage critical point for each Ti-indenyl side of the metallocene which are not associated to any ring and cage, respectively. Although its virial graph also shows just one Ti–C bond path for each indenyl ligand, the virial path links C2 to Ti instead of C1 to Ti, as it happens in the corresponding molecular graph, and C6–Ti virial path is about to become a BCP–Ti virial path, indicating a three-center bonding (Ti–C–C6). Then, possibly there are two bond paths between each indenyl ligand and Ti atom in $Ind_2Ti(CH_3)_2$ instead of just one.

Table 2
Values of electronic energy change of reaction (in kcal/mol) from the global synthesis reaction of Ind_2TiMe_2 and Cp_2TiMe_2 and their corresponding relation with the number of bond paths between each π-ligand and Ti atom.

Global reaction	Number of bond paths between each π-ligand and Ti atom	Electronic energy change of reaction (kcal/mol)
$TiCl_4 + 2IndLi + 2MeLi \rightarrow Ind_2TiMe_2 + 4LiCl$	1 or 2	−42.5
$TiCl_4 + 2CpLi + 2MeLi \rightarrow Cp_2TiMe_2 + 4LiCl$	3	−50.0

The interatomic distances between C atom (from cyclopentadienyl group of indenyl ligand) and Ti atom are rather different from one another and only the smallest one (with 2.364 Å – Figure 2) has a corresponding bond path. Accordingly, C1–Ti atomic pair have the highest value of DI while other Ti–C (from the indenyl ligand) atomic pairs have smaller DI values (see Figure 4). In a comparison of atomic charge and atomic energy values between C1 and C3 atoms, where C1 has a Ti–C bond path and C3 not, the C1 atom has smaller atomic energy and more negative atomic charge than those from C3, indicating that the bond path is related to a higher stability of C1 atom (Figure 4).

The dimethyl-bis(indenyl) titanium has fewer quantity of bond paths involving Ti–C atoms (2 or 4 bond paths) than that from dimethyl-bis(cyclopentadienyl) titanium (6 bond paths). These QTAIM results indicate that the bent titanocene with indenyl ligands is less stable than the bent titanocene with cyclopentadienyl ligands. In Table 2 there are values of electronic energy change of reaction for the global synthesis reactions of $Cp_2Ti(CH_3)_2$ and $Ind_2Ti(CH_3)_2$ which agree with QTAIM results related to the number of bonded interactions between carbon and titanium atoms. These theoretical results are also in agreement with experimental observations about their stabilities.

6. Conclusions

The topological data of the bond critical points of Ti–C bond paths involving cyclopentadienyl or indenyl ligands are nearly characteristic of closed shell interactions (ionic bond) while the interaction of the Ti–C bond from σ-methyl group is intermediate between ionic and covalent bond. This means that one σ-methyl ligand has stronger interaction with Ti atom than one interaction from π-cyclopentadienyl ligand with Ti atom.

Based on the quantity of bond paths between titanium and carbon atoms, the dimethyl-bis(indenyl) titanium is less stable than the dimethyl-bis(cyclopentadienyl) titanium since the former has fewer number of bond paths than the latter.

For the studied molecular systems we can state that the number of bond paths can be used as an indicative of stability of metallocenes. The carbon atoms of π-ligands linked to Ti atom by a bond path are more stable than those which does not have C–Ti bond path, regardless their corresponding C–Ti DI values.

Acknowledgments

Authors thank FAPERJ, CAPES and CNPq for financial support.

References

[1] R.H. Crabtree, The Organometallic Chemistry of the Transition Metals, John Wiley and Sons, Hoboken, New Jersey, 2005.
[2] J.C.W. Chien, J. Phys. Chem. 67 (1963) 2477.
[3] C. Lecomte, Y. Dusausoy, J. Protas, J. Tirouflet, A. Dormond, J. Organomet. Chem. 73 (1974) 67.
[4] H.G. Alt, A. Koppl, Chem. Rev. 100 (2000) 1205.
[5] L. Resconi, L. Cavallo, A. Fait, F. Piemontesi, Chem. Rev. 100 (2000) 1253.
[6] J.A. Ewen, J. Am. Chem. Soc. 106 (1984) 6355.
[7] M. Bochmann, J. Chem. Soc., Dalton Trans. (1996) 255.
[8] J.L. Petersen, L.F. Dahl, J. Am. Chem. Soc. 97 (1975) 6422.
[9] Z.T. Tsai, C.H. Brubaker, J. Organomet. Chem. 166 (1979) 199.
[10] E. Vitz, P.J. Wagner, C.H. Brubaker, J. Organomet. Chem. 107 (1976) 301.
[11] E. Vitz, C.H. Brubaker, J. Organomet. Chem. 82 (1974) C16.
[12] G. Guerra, L. Cavallo, G. Moscardi, M. Vacatello, P. Corradini, Macromolecules 29 (1996) 4834.
[13] G. Guerra, L. Cavallo, G. Moscardi, M. Vacatello, P. Corradini, J. Am. Chem. Soc. 116 (1994) 2988.
[14] L. Cavallo, G. Guerra, M. Vacatello, P. Corradini, Macromolecules 24 (1991) 1784.
[15] V. Venditto, G. Guerra, P. Corradini, R. Fusco, Polymer 31 (1990) 530.
[16] V. Busico, R. Cipullo, J.C. Chadwick, J.F. Modder, O. Sudmeijer, Macromolecules 27 (1994) 7538.
[17] A.V. Grafov, C.L. Firme, I.A. Grafova, F. Benetollo, M.L. Dias, M.J.M. Abadie, Polymer 46 (2005) 9626.
[18] C.L. Firme, A.V. Grafov, M.L. Dias, J. Polym. Sci., Part A: Polym. Chem. 43 (4248) (2005).
[19] M.L. Dias, D.E.B. Lopes, A.V. Grafov, J. Mol. Catal. A: Chem. 185 (2002) 57.
[20] D.E.B. Lopes, M.L. Dias, M.F.V. Marques, A.V. Grofov, Polym. Bull. 45 (2000) 365.
[21] C.E. Zachmanoglou et al., J. Am. Chem. Soc. 124 (2002) 9525.
[22] X.J. Wang, L. Chen, A. Endou, M. Kubo, A. Miyamoto, J. Organomet. Chem. 678 (2003) 156.
[23] S.A. Kozimor et al., Inorg. Chem. 47 (2008) 5365.
[24] M.A. Freitag, M.S. Gordon, J. Phys. Chem. A 106 (2002) 7921.
[25] S.K. Ignatov, N.H. Rees, B.R. Tyrrell, S.R. Dubberley, A.G. Razuvaev, P. Mountford, G.I. Nikonov, Chem. Eur. J. 10 (2004) 4991.
[26] F. Cortés-Guzmán, R.F.W. Bader, Coord. Chem. Rev. 249 (2005) 633.
[27] I. Vidal, S. Melchor, J.A. Dobado, J. Phys. Chem. A 112 (2008) 3414.
[28] R. Fletcher, Practical Methods of Optimization, Wiley, New York, 1980.
[29] J.P. Perdew, K. Burke, M. Ernzerhof, Phys. Rev. Lett. 77 (1996) 3865.
[30] J.P. Perdew, K. Burke, M. Ernzerhof, Phys. Rev. Lett. 80 (1998) 891.
[31] R. Krishnan, J.S. Binkley, R. Seeger, J.A. Pople, J. Chem. Phys. 72 (1980) 650.
[32] M.J. Frisch et al., Gaussian 03. Revision B.04, Gaussian Inc., Pittsburgh, 2003.
[33] F. Biegler-König, J. Schönbohm, AIM 2000 (2002).
[34] R.F.W. Bader, Atoms in Molecules a Quantum Theory, Oxford, Oxford, 1994.
[35] P.L.A. Popelier, Atoms in Molecules An Introduction, Prentice Hall, Manchester, 2000.
[36] R.F.W. Bader, M.E. Stephens, J. Am. Chem. Soc. 97 (1975) 7391.
[37] R.F.W. Bader, A. Streitwieser, A. Neuhaus, K.E. Laidig, P. Speers, J. Am. Chem. Soc. 118 (1996) 4959.
[38] T. Koritsanszky, J. Buschmann, P. Luger, J. Phys. Chem. 100 (1996) 10547.
[39] T.S. Koritsanszky, P. Coppens, Chem. Rev. 101 (2001) 1583.
[40] C.F. Matta, R.F.W. Bader, J. Phys. Chem. A 110 (2006) 6365.
[41] C.L. Firme, O.A.C. Antunes, P.M. Esteves, Chem. Phys. Lett. 468 (2009) 129.
[42] G.N. Lewis, J. Am. Chem. Soc. 38 (1916) 762.
[43] C.A. Tolman, Chem. Soc. Rev. 1 (1972) 337.
[44] P. Balanarayan, S.R. Gadre, J. Chem. Phys. 119 (2003) 5037.
[45] R.F.W. Bader, J. Phys. Chem. A 102 (1998) 7314.
[46] P.v.R. Schleyer, R.C. Fort Jr., W.E. Watts, M.B. Comisaro, G.A. Olah, J. Am. Chem. Soc. 86 (4195) (1964).
[47] G. Wilkinson, M. Rosenblum, M.C. Whiting, R.B. Woodward, J. Am. Chem. Soc. 74 (1952) 2125.
[48] J.L. Atwood, W.E. Hunter, D.C. Hrncir, E. Samuel, H. Alt, M.D. Rausch, Inorg. Chem. 14 (1975) 1757.